



Cadmium(II)-imidazolylazo dyes: Synthesis, structure and photochromism

S. Saha (Halder)^{a,1}, B.G. Chand^d, J.-S. Wu^b, T.-H. Lu^b, P. Raghavaiah^c, C. Sinha^{a,*}

^a Department of Chemistry, Inorganic Chemistry Section, Jadavpur University, Kolkata 700 032, India

^b Department of Physics, National Tsing Hua University, Hsinchu 300, Taiwan, ROC

^c School of Chemistry, National Single Crystal X-ray Diffractometer Facility, University of Hyderabad, Hyderabad 500 046, India

^d School of Education, Basantapur Education Society, Domkal, Murshidabad, India

ARTICLE INFO

Article history:

Received 28 April 2012

Accepted 16 July 2012

Available online 27 July 2012

Keywords:

Cd(II)-thioalkylphenyl-azoimidazole

Distorted Td-symmetry

Photochromism

Activation energy

Effect of halide

ABSTRACT

1-Alkyl-2-((*o*-thioalkyl)phenylazo)imidazole acts as imidazolyl-N donor ligand to Cd(II) although they have potential three donor centres namely N(imidazole), N(azo) and –SR. Two series of complexes [Cd(SRaaNR')₂X₂] (X = Cl, Br, I) and [Cd(SRaaNR')₄](ClO₄)₂ are synthesized with these ligands. These complexes are spectroscopically (IR, UV–Vis, ¹H NMR) characterised and, the single crystal X-ray structures of [Cd(SEtaaiNEt)₂I₂] and [Cd(SEtaaiNEt)₄](ClO₄)₂ (where SEtaaiNEt = 1-ethyl-2-((*o*-thioalkyl)phenylazo)imidazole) have confirmed the distorted tetrahedral structures. The UV light irradiation in MeCN solution of the complexes shows *E*-to-*Z* (*E* and *Z* refer to *trans* and *cis*-configuration about –N=N–, respectively) isomerisation of the coordinated azoimidazole. The rate of isomerisation follows the sequence : [Cd(SRaaNR')₄](ClO₄)₂ < [Cd(SRaaNR')₂Cl₂] < [Cd(SRaaNR')₂Br₂] < [Cd(SRaaNR')₂I₂]. Quantum yields ($\phi_{E \rightarrow Z}$) and the activation energy (E_a) of the isomerisation of the complexes are lower than that of free ligand data. The observation has been explained considering the molecular association that increases the mass and rotor volume of the complexes.

© 2012 Elsevier Ltd. All rights reserved.

1. Introduction

Cadmium and its compounds have some importance in social perspective. Main application of cadmium is in rechargeable batteries and photoconducting devices [1]. Cadmium may cause major pathological effects on the kidneys. Because of borderline acidity cadmium(II) can bind strongly imidazole and may hamper biochemical reactions since most of the biomolecules have imidazole unit [2]. This has created interest to study the coordination chemistry of Cd(II)-imidazole/imidazole containing ligands [3]. We have synthesized series of ligands belong to azo dyes, 1-alkyl-2-(arylazo)imidazoles (RaaNR', **1**) and have characterised many of their metal complexes [4,5]. The functionalization to pendant aryl group has been done by *ortho* –SR substitution to synthesize 1-alkyl-2-((*o*-thioalkyl)phenylazo)imidazoles (**2**) [6]. These ligands have potentially three coordination centres – imidazole-N (N), azo-N (N') and thioether-S (–SR). The ligand shows both tridentate N, N', S [12] and bidentate N, N' chelation [7].

Arylazoimidazoles and some of their coordination complexes show reversible transformation between *trans*-form and *cis*-form upon UV light irradiation [8–11]. The phenomenon is defined as photochromism. The photochromic compounds have attracted

much recent interest because of their potential applications in different areas such as liquid crystal alignment [12], optical data storage [13], non-linear optics [14], photoswitching [15] and molecular-photonics devices [16]. Photochromic compounds have distinct absorption spectral change when excited at least in one pathway by light. One of the important problems of organic photochrome is “fatigue” and low durability where “fatigue” refers to photodegradation, photobleaching, photooxidation, and other chemical degradation and physical deformation or side reactions. The attachment of a metal ion to photochromic organic compounds such as azobenzene derivatives or diarylethens can reduce fatigue and enhances the stability of the excited states. In continuation of our effort, this work refers to the photoisomerisation of the cadmium(II)-SRaaNR' complexes. The ligand is hooked to Cd(II) via imidazolyl-N coordination and the hanging thioalkyl-arylazoimidazole undergoes reversible photoisomerisation. Ligand, SRaaNR', has three potential donor centres – N(imidazole), N(azo) and –S-R and can serve as tridentate-N,N',S [6] and bidentate-N,N' [7] donor agents. The single crystal X-ray structure determination of representative complexes show monodentate ligating behaviour of SRaaNR' to Cd(II) and may be more flexible to isomerisation by light irradiation relative to the chelated system [6,7]. The effect of Cd-X (X = Cl, Br, I) and number of coordinated SRaaNR' on photoisomerisation rate and quantum yields have been discussed along with the addition of excess cadmium(II) salt.

* Corresponding author. Fax: +91 2414 6584.

E-mail address: c_r_sinha@yahoo.com (C. Sinha).

¹ Present address: Department of Chemistry, Kalyani Govt. Engg. College, India

2. Experimental

2.1. Material

CdCl₂, CdBr₂ and CdI₂ were obtained from Loba Chemicals, Bombay, India 1-alkyl-2-((*o*-thio alkyl)phenyl azo)imidazole were synthesized by reported procedure [6]. All other chemicals and solvents were reagent grade as received. Cd(ClO₄)₂ 6H₂O was prepared from CdCO₃ and perchloric acid.

2.2. Physical measurements

Microanalytical data (C, H, N) were collected on Perkin-Elmer 2400 CHNS/O elemental analyzer. Spectroscopic data were obtained using the following instruments: UV–Vis spectra from a Perkin Elmer Lambda 25 spectrophotometer; IR spectra (KBr disk, 4000–200 cm⁻¹) from a Perkin Elmer RX-1 FTIR spectrophotometer; photoexcitation has been carried out using a Perkin Elmer LS-55 spectrofluorimeter and ¹H NMR spectra from a Bruker (AC) 300 MHz FTNMR spectrometer.

2.3. Synthesis

2.3.1. Synthesis of [Cd(SEtaaiNet)₂l₂] (5d)

1-Ethyl-2-((*o*-thioethyl)phenylazo)imidazole (43 mg, 0.17 mmol) in CH₃CN was added in drops to MeOH solution of CdI₂ (30 mg, 0.08 mmol) was stirred for 2 h. The resultant reddish solution was collected by filtration; slow evaporation of the solution gives the red crystal. The yield was 46.46 mg (64%). Other complexes were prepared under identical conditions from MeOH/MeCN solution and the yield varied in the range 60–70%.

Microanalytical data of the complexes are as follows: [Cd(SMeaiiNMe)₂Cl₂] (**3a**) Found: C, 40.8; H, 3.6; N, 17.31%. *Anal. Calc.* for C₂₂H₂₄N₈S₂Cl₂Cd C, 40.79; H, 3.7; N, 17.30. FT-IR (KBr disc, cm⁻¹), ν(N=N), 1426; ν(C=N), 1660 cm⁻¹. UV–Vis spectroscopic data in CH₃CN (λ_{max}(nm) (10⁻³ ∈ (dm³ mol⁻¹cm⁻¹)): 372 (23), 415 (20). ¹H NMR (300 MHz, CDCl₃), δ(ppm), (J(Hz)): 7.41 (bs, 4-H), 7.24 (bs, 5-H), 7.35 (d, 7.00 Hz, 8-H), 7.44 (m, 9- and 10-H), 8.10 (d, 8.00 Hz, 11-H), 4.32 (s, 1-CH₃), 2.60 (s, S-CH₃). [Cd(SMeaiiNET)₂Cl₂] (**3b**) Found: C, 42.66; H, 4.15; N, 16.56%. *Anal. Calc.* for C₂₄H₂₈N₈S₂Cl₂Cd C, 42.65; H, 4.14; N, 16.58. FT-IR (KBr disc, cm⁻¹), ν(N=N), 1420; ν(C=N), 1662 cm⁻¹. UV–Vis spectroscopic data in CH₃CN (λ_{max}(nm) (10⁻³ ∈ (dm³ mol⁻¹cm⁻¹)): 372 (26), 414 (22). ¹H NMR (300 MHz, CDCl₃), δ(ppm), (J(Hz)): 7.42 (bs, 4-H), 7.23 (bs, 5-H), 7.32 (d, 7.00 Hz, 8-H), 7.43 (m, 9- and 10-H), 7.98 (d, 8.00 Hz, 11-H), 4.48 (q, 6.62 Hz, 1-CH₂), 1.65 (t, 7.27 Hz, (1-CH₂)-CH₃), 2.67 (s, S-CH₃). [Cd(SEtaaiNMe)₂Cl₂] (**3c**) Found: C, 42.67; H, 4.13; N, 16.57%. *Anal. Calc.* for C₂₄H₂₈N₈S₂Cl₂Cd C, 42.65; H, 4.14; N, 16.58. FT-IR (KBr disc, cm⁻¹), ν(N=N), 1427; ν(C=N), 1660 cm⁻¹. UV–Vis spectroscopic data in CH₃CN (λ_{max}(nm) (10⁻³ ∈ (dm³ mol⁻¹cm⁻¹)): 378 (23.35), 414 (25.56). ¹H NMR (300 MHz, CDCl₃), δ(ppm), (J(Hz)): 7.40 (bs, 4-H), 7.23 (bs, 5-H), 7.34 (d, 7.00 Hz, 8-H), 7.46 (m, 9- and 10-H), 7.94 (d, 7.90 Hz, 11-H), 4.28 (s, 1-CH₃), 3.01 (q, 7.20 Hz, S-CH₂), 1.31 (t, 7.35 Hz, (S-CH₂)-CH₃). [Cd(SEtaaiNET)₂Cl₂] (**3d**) Found: C, 44.35; H, 4.55; N, 15.93%. *Anal. Calc.* for C₂₆H₃₂N₈S₂Cl₂Cd C, 44.36; H, 4.54; N, 15.92. FT-IR (KBr disc, cm⁻¹), ν(N=N), 1428; ν(C=N), 1661 cm⁻¹. UV–Vis spectroscopic data in CH₃CN (λ_{max}(nm) (10⁻³ ∈ (dm³ mol⁻¹cm⁻¹)): 371 (32.58), 413 (28.86). ¹H NMR (300 MHz, CDCl₃), δ(ppm), (J(Hz)): 7.41 (bs, 4-H), 7.22 (bs, 5-H), 7.35 (d, 7.00 Hz), 7.45 (m, 9- and 10-H), 7.97 (d, 8.00 Hz, 11-H), 4.59 (q, 6.68 Hz, 1-CH₂), 1.60 (t, 7.23 Hz, (1-CH₂)-CH₃), 3.04 (q, 7.20 Hz, S-CH₂), 1.39 (t, 7.36 Hz, (S-CH₂)-CH₃). [Cd(SMeaiiNMe)₂Br₂] (**4a**) Found: C, 35.86; H, 3.22; N, 15.20%. *Anal. Calc.* for C₂₂H₂₄N₈S₂Br₂Cd C, 35.85; H, 3.25; N, 15.21. FT-IR (KBr disc, cm⁻¹), ν(N=N), 1415;

ν(C=N), 1646 cm⁻¹. UV–Vis spectroscopic data in CH₃CN (λ_{max}(nm) (10⁻³ ∈ (dm³ mol⁻¹cm⁻¹)): 371 (22.15), 414 (19.06). ¹H NMR (300 MHz, CDCl₃), δ(ppm), (J(Hz)): 7.40 (bs, 4-H), 7.23 (bs, 5-H), 7.36 (d, 7.00 Hz, 11-H), 7.55 (m, 9- and 10-H), 7.84 (d, 8.00 Hz), 4.72 (s, 1-CH₃), 2.55 (s, S-CH₃). [Cd(SMeaiiNET)₂Br₂] (**4b**) Found: C, 37.69; H, 3.67; N, 14.62%. *Anal. Calc.* for C₂₄H₂₈N₈S₂Br₂Cd C, 37.68; H, 3.66; N, 14.65. FT-IR (KBr disc, cm⁻¹), ν(N=N), 1416; ν(C=N), 1645 cm⁻¹. UV–Vis spectroscopic data in CH₃CN (λ_{max}(nm) (10⁻³ ∈ (dm³ mol⁻¹cm⁻¹)): 372 (28), 414 (22.01). ¹H NMR (300 MHz, CDCl₃), δ(ppm), (J(Hz)): 7.41 (bs, 4-H), 7.20 (bs, 5-H), 7.33 (d, 7.00 Hz, 8-H), 7.52 (m, 9- and 10-H), 7.88 (d, 8.00 Hz, 11-H), 4.47 (q, 7.00 Hz, 1-CH₂), 1.69 (t, 7.29 Hz, (1-CH₂)-CH₃), 2.64 (s, S-CH₃). [Cd(SEtaaiNMe)₂Br₂] (**4c**) Found: C, 37.67; H, 3.65; N, 14.63%. *Anal. Calc.* for C₂₄H₂₈N₈S₂Br₂Cd C, 37.68; H, 3.66; N, 14.65. FT-IR (KBr disc, cm⁻¹), ν(N=N), 1416; ν(C=N), 1645 cm⁻¹. UV–Vis spectroscopic data in CH₃CN (λ_{max}(nm) (10⁻³ ∈ (dm³ mol⁻¹cm⁻¹)): 373 (27), 415 (22.3). ¹H NMR (300 MHz, CDCl₃), δ(ppm), (J(Hz)): 7.42 (bs, 4-H), 7.20 (bs, 5-H), 7.35 (d, 7.00 Hz, 8-H), 7.56 (m, 9- and 10-H), 7.83 (d, 8.05 Hz, 11-H), 4.30 (s, 1-CH₃), 3.00 (q, 7.35 Hz, S-CH₂), 1.30 (6.17 Hz, (S-CH₂)-CH₃). [Cd(SEtaaiNET)₂Br₂] (**4d**) Found: C, 39.39; H, 4.0; N, 14.12%. *Anal. Calc.* for C₂₆H₃₂N₈S₂Br₂Cd C, 39.38; H, 4.03; N, 14.13. FT-IR (KBr disc, cm⁻¹), ν(N=N), 1428; ν(C=N), 1649 cm⁻¹. UV–Vis spectroscopic data in CH₃CN (λ_{max}(nm) (10⁻³ ∈ (dm³ mol⁻¹cm⁻¹)): 373 (29.56), 415 (28.62). ¹H NMR (300 MHz, CDCl₃), δ(ppm), (J(Hz)): 7.41 (bs, 4-H), 7.22 (bs, 5-H), 7.32 (d, 7.00 Hz), 7.53 (m, 9- and 10-H), 7.86 (d, 8.00 Hz, 11-H), 4.52 (q, 7.25 Hz, 1-CH₂), 1.62 (t, 7.24 Hz, (1-CH₂)-CH₃), 3.04 (q, 7.30 Hz, S-CH₂), 1.35 (t, 6.16 Hz, (S-CH₂)-CH₃). [Cd(SMeaiiNMe)₂I₂] (**5a**) Found: C, 31.75; H, 2.84; N, 13.52. *Anal. Calc.* for C₂₂H₂₄N₈S₂I₂Cd C, 31.79; H, 2.89; N, 13.49. FT-IR (KBr disc, cm⁻¹), ν(N=N), 1417; ν(C=N), 1619 cm⁻¹. UV–Vis spectroscopic data in CH₃CN (λ_{max}(nm) (10⁻³ ∈ (dm³ mol⁻¹cm⁻¹)): 373 (18.26), 415 (16.92). ¹H NMR (300 MHz, CDCl₃), δ(ppm), (J(Hz)): 7.41 (bs, 4-H), 7.28 (bs, 5-H), 7.31 (d, 7.00 Hz, 11-H), 7.55 (m, 9- and 10-H), 7.80 (d, 8.00 Hz), 4.14 (s, 1-CH₃), 2.52 (s, S-CH₃). [Cd(SMeaiiNET)₂I₂] (**5b**) Found: C, 33.57; H, 3.20; N, 13.1. *Anal. Calc.* for C₂₄H₂₈N₈S₂I₂Cd C, 33.55; H, 3.26; N, 13.05. FT-IR (KBr disc, cm⁻¹), ν(N=N), 1428; ν(C=N), 1622 cm⁻¹. UV–Vis spectroscopic data in CH₃CN (λ_{max}(nm) (10⁻³ ∈ (dm³ mol⁻¹cm⁻¹)): 372 (27.05), 416 (21.59). ¹H NMR (300 MHz, CDCl₃), δ(ppm), (J(Hz)): 7.40 (bs, 4-H), 7.23 (bs, 5-H), 7.34 (d, 7.00 Hz, 8-H), 7.56 (m, 9- and 10-H), 7.82 (d, 8.00 Hz, 11-H), 4.51 (q, 7.00 Hz, 1-CH₂), 1.63 (t, 7.30 Hz, (1-CH₂)-CH₃), 2.59 (s, S-CH₃). [Cd(SEtaaiNMe)₂I₂] (**5c**) Found: C, 33.47; H, 3.0; N, 13.00%. *Anal. Calc.* for C₂₄H₂₈N₈S₂I₂Cd C, 33.49; H, 3.10; N, 13.05. FT-IR (KBr disc, cm⁻¹), ν(N=N), 1427; ν(C=N), 1620 cm⁻¹. UV–Vis spectroscopic data in CH₃CN (λ_{max}(nm) (10⁻³ ∈ (dm³ mol⁻¹cm⁻¹)): 371 (26.00), 414 (22.30). ¹H NMR (300 MHz, CDCl₃), δ(ppm), (J(Hz)): 7.43 (bs, 4-H), 7.27 (bs, 5-H), 7.32 (d, 7.00 Hz, 8-H), 7.55 (m, 9- and 10-H), 7.81 (d, 8.05 Hz, 11-H), 4.17 (s, 1-CH₃), 3.00 (q, 7.30 Hz, S-CH₂), 1.29 (t, 7.00 Hz, (S-CH₂)-CH₃). [Cd(SEtaaiNET)₂I₂] (**5d**) Found: C, 35.1; H, 3.62; N, 12.64%. *Anal. Calc.* for C₂₆H₃₂N₈S₂I₂Cd C, 35.20; H, 3.61; N, 12.63. FT-IR (KBr disc, cm⁻¹), ν(N=N), 1427; ν(C=N), 1620 cm⁻¹. UV–Vis spectroscopic data in CH₃CN (λ_{max}(nm) (10⁻³ ∈ (dm³ mol⁻¹cm⁻¹)): 372 (26.10), 412 (24.35). ¹H NMR (300 MHz, CDCl₃), δ(ppm), (J(Hz)): 7.42 (bs, 4-H), 7.22 (bs, 5-H), 7.33 (d, 7.00 Hz), 7.56 (m, 9- and 10-H), 7.80 (d, 8.10 Hz, 11-H), 4.44 (q, 7.25 Hz, 1-CH₂), 1.61 (t, 7.25 Hz, (1-CH₂)-CH₃), 3.05 (q, 7.40 Hz, S-CH₂), 1.30 (t, 5.25 Hz, (S-CH₂)-CH₃).

2.3.2. Synthesis of [Cd(SEtaaiNET)₄](ClO₄)₂ (6d)

1-Ethyl-2-((*o*-thioethyl)phenylazo)imidazole (86 mg, 0.32 mmol) in MeOH was added in drops to aqueous solution of Cd(ClO₄)₂ 6 H₂O (30 mg, 0.08 mmol) was stirred for 2 h. The resultant reddish solution was collected by filtration; slow evaporation of the solution gives the red crystal. The yield was 61.87 mg (64%). Other

Table 1
Summarized crystallographic data for [Cd(SEtaaiNet)₂]₂ (**5d**) and [Cd(SEtaaiNet)₄](ClO₄)₂ (**6d**).

Parameters	[Cd(SEtaaiNet) ₂] ₂ (5d)	[Cd(SEtaaiNet) ₄](ClO ₄) ₂ (6d)
Empirical formula	C ₂₆ H ₃₂ N ₈ S ₂ I ₂ Cd	C ₅₂ H ₆₄ N ₁₆ O ₈ S ₄ Cl ₂ Cd
Formula weight	886.92	1352.79
Temperature (K)	100(2)	295(2)
Crystal system	monoclinic	triclinic
Space group	<i>P</i> 2 ₁ / <i>n</i>	<i>P</i> $\bar{1}$
Crystal size (mm)	0.20 × 0.20 × 0.10	0.20 × 0.10 × 0.10
<i>Unit cell dimensions</i>		
<i>a</i> (Å)	15.598(3)	12.5810(9)
<i>b</i> (Å)	11.355(2)	13.2964(9)
<i>c</i> (Å)	19.700(4)	19.5999(13)
α (°)	90.00	75.0500(10)
β (°)	111.998(5)	83.8280(10)
γ (°)	90.00	82.2740(10)
<i>V</i> (Å ³)	3235.3(10)	3129.9(4)
<i>Z</i>	4	2
λ (Å)	0.71073	0.71073
μ (Mo-K α) (mm ⁻¹)	2.742	0.631
<i>D</i> _{calc} (mgm ⁻³)	1.821	1.435
<i>hkl</i> Range	-15 ≤ <i>h</i> ≤ 19, -14 ≤ <i>k</i> ≤ 14, -24 ≤ <i>l</i> ≤ 24	-16 ≤ <i>h</i> ≤ 16, -17 ≤ <i>k</i> ≤ 17, -25 ≤ <i>l</i> ≤ 26
θ Range (°)	1.43–26.37	1.08–28.33
Refine parameters	356	748
Unique data [<i>I</i> > 2 σ (<i>I</i>)]	6599	4517
<i>R</i> ₁ ^a [<i>I</i> > 2 σ (<i>I</i>)]	0.0420	0.0456
<i>wR</i> ₂ ^b	0.1283	0.1147
Goodness of fit	1.07	0.693

^a $R = \sum |F_o - F_c| / \sum F_o$.

^b $wR = [\sum w(F_o^2 - F_c^2)^2 / \sum wF_o^4]^{1/2}$ are general but *w* are different, $w = 1/[\sigma^2(F^2) + (0.0527P)^2 + 2.3556P]$ for (**5d**); $w = 1/[\sigma^2(F^2) + (0.0980P)^2]$ for (**6d**) where $P = (F_o^2 + 2F_c^2)/3$.

complexes were prepared under identical conditions from MeOH/H₂O solution and the yield varied in the range 60–70%.

[Cd(SMeaiiNMe)₄](ClO₄)₂ (**6a**) Found: C, 42.61; H, 3.86; N, 18.08%. *Anal. Calc.* for C₄₄H₄₈N₁₆S₄C₁₂O₈Cd C, 42.60; H, 3.87; N, 18.07. FT-IR (KBr disc, cm⁻¹), ν (N=N), 1423; ν (C=N), 1651 cm⁻¹, ν (ClO₄), 1088–1118 cm⁻¹ UV-Vis spectroscopic data in CH₃CN (λ_{\max} (nm)(10⁻³ ∈ (dm³ mol⁻¹cm⁻¹): 371 (78.85), 413(61.55). ¹H NMR (300 MHz, CDCl₃), δ (ppm), (J(Hz)): 7.10 (bs, 4-H), 6.92 (bs, 5-H), 6.98 (d, 7.00 Hz, 11-H), 7.47 (m, 9- and 10-H), 7.73 (d, 8.00 Hz), 4.18 (s, 1-CH₃), 2.54 (s, S-CH₃). [Cd(SMeaiiNet)₄](ClO₄)₂ (**6b**) Found: C, 44.48; H, 4.33; N, 17.28%. *Anal. Calc.* for C₄₈H₅₆N₁₆S₄C₁₂O₈Cd C, 44.47; H, 4.32; N, 17.29. FT-IR (KBr disc, cm⁻¹), ν (N=N), 1426; ν (C=N), 1655 cm⁻¹, ν (ClO₄), 1087–1088 cm⁻¹ UV-Vis spectroscopic data in CH₃CN (λ_{\max} (nm)(10⁻³ ∈ (dm³ mol⁻¹cm⁻¹): 373 (68), 415 (62.21). ¹H NMR (300 MHz, CDCl₃), δ (ppm), (J(Hz)): 7.12 (bs, 4-H), 6.95 (bs, 5-H), 7.00 (d, 7.00 Hz, 8-H), 7.46 (m, 9- and 10-H), 7.71 (d, 8.00 Hz, 11-H), 4.481 (q, 7.00 Hz, 1-CH₂), 1.52 (t, 7.20 Hz, (1-CH₂)-CH₃), 2.52 (s, S-CH₃). [Cd(SEtaaiNMe)₄](ClO₄)₂ (**6c**) Found: C, 44.46; H, 4.31; N, 17.3%. *Anal. Calc.* for C₄₈H₅₆N₁₆S₄C₁₂O₈Cd C, 44.47; H, 4.32; N, 17.29. FT-IR (KBr disc, cm⁻¹), ν (N=N), 1425; ν (C=N), 1653 cm⁻¹, ν (ClO₄), 1088 cm⁻¹ UV-Vis spectroscopic data in CH₃CN (λ_{\max} (nm)(10⁻³ ∈ (dm³ mol⁻¹cm⁻¹): 372 (65), 413 (66). ¹H NMR (300 MHz, CDCl₃), δ (ppm), (J(Hz)): 7.09 (bs, 4-H), 6.90 (bs, 5-H), 6.97 (d, 7.00 Hz, 8-H), 7.45 (m, 9- and 10-H), 7.67 (d, 8.00 Hz, 11-H), 4.15 (s, 1-CH₃), 2.70 (q, 7.30 Hz, S-CH₂), 1.23 (t, 7.00 Hz, (S-CH₂)-CH₃). [Cd(SEtaaiNet)₄](ClO₄)₂ (**6d**) Found: C, 46.16; H, 4.74; N, 16.55%. *Anal. Calc.* for C₅₂H₆₄N₁₆S₄C₁₂O₈Cd C, 46.17; H, 4.73; N, 16.57. FT-IR (KBr disc, cm⁻¹), ν (N=N), 1427; ν (C=N), 1652 cm⁻¹, ν (ClO₄),

1089–1114 cm⁻¹ UV-Vis spectroscopic data in CH₃CN (λ_{\max} (nm)(10⁻³ ∈ (dm³ mol⁻¹cm⁻¹): 371 (49.26), 411 (39.76). ¹H NMR (300 MHz, CDCl₃), δ (ppm), (J(Hz)): 7.09 (bs, 4-H), 6.90 (bs, 5-H), 6.98 (d, 7.00 Hz), 7.43 (m, 9- and 10-H), 7.66 (d, 8.10 Hz, 11-H), 4.46 (q, 7.10 Hz, 1-CH₂), 1.46 (t, 7.20 Hz, (1-CH₂)-CH₃), 2.96 (q, 7.30 Hz, S-CH₂), 1.26 (t, 5.50 Hz, (S-CH₂)-CH₃).

2.4. X-ray diffraction study

Single crystals suitable for data collection were grown from slow evaporation of DMF solution of the complexes in methanol. The crystal data and details of the data collections are given in Table 1. A suitable single crystal of the complexes (**5d**: 0.20 × 0.20 × 0.10 mm and **6d**: 0.20 × 0.10 × 0.10 mm) was mounted on a Bruker SMART APEX CCD diffractometer (graphite monochromated MoK α radiation, $\lambda = 0.71073$ Å) and data were collected by use of ω scans. Unit cell parameters were determined from least-squares refinement of setting angles (θ) within the range $1.43 \leq \theta \leq 26.37^\circ$ (**5d**) and $1.08 \leq \theta \leq 28.33^\circ$ (**6d**). Data were corrected for Lorentz polarisation effects and for linear decay. Semi-empirical absorption corrections based on Ψ -scans were applied. The structures were solved by direct method using SHELXS-97 [17] and successive difference Fourier syntheses. All non-hydrogen atoms were refined anisotropically. The hydrogen atoms were fixed geometrically and refined using the riding model. All calculation was carried out using SHELXL-97 [18], ORTEP-32 [19] and PLATON-99 [20] programs.

2.5. Photometric measurements

Absorption spectra were taken with a PerkinElmer Lambda 25 UV/VIS Spectrophotometer in a 1 × 1 cm quartz optical cell maintained at 25 °C with a Peltier thermostat. The light source of a PerkinElmer LS 55 spectrofluorimeter was used as an excitation light, with a slit width of 10 nm. An optical filter was used to cut off overtones when necessary. The absorption spectra of the *cis* isomers were obtained by extrapolation of the absorption spectra of a *cis*-rich mixture for which the composition is known from ¹H NMR integration. Quantum yields (ϕ) were obtained by measuring initial *trans*-to-*cis* isomerization rates (ν) in a well-stirred solution within the above instrument using the equation,

$$\nu = (\phi I_0 / V)(1 - 10^{-Abs}).$$

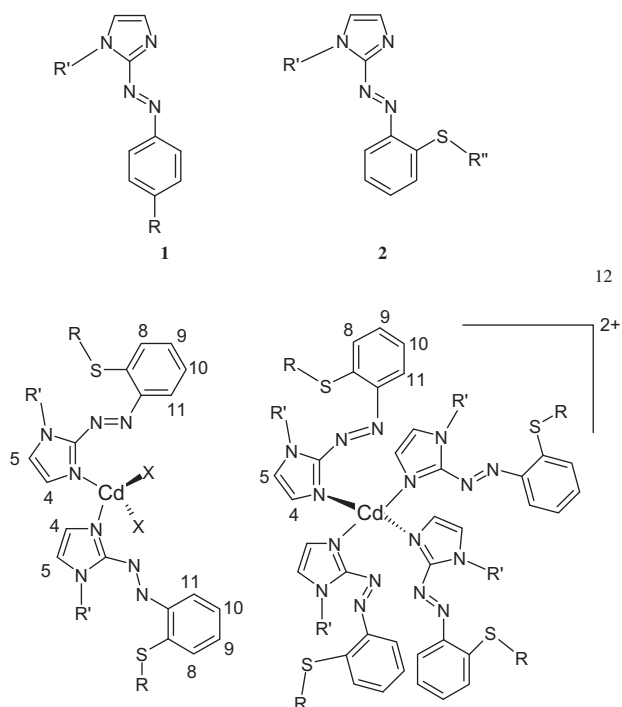
where I_0 is the photon flux at the front of the cell, V is the volume of the solution, and Abs is the initial absorbance at the irradiation wavelength. The value of I_0 was obtained by using azobenzene ($\phi = 0.11$ for $\pi - \pi^*$ excitation [21]) under the same irradiation conditions.

The *Z*-to-*E* isomerisation has been carried out at temperature range 298–321 K. The rates of thermal isomerisation were obtained by monitoring absorption changes intermittently for a *cis*-rich solution kept in the dark at constant temperatures (298–321 K). The activation energy (E_a) and the frequency factor (A) were obtained from the Arrhenius plot, $\ln k = \ln A - E_a/RT$ where k is the measured rate constant, R is the gas constant, and T is temperature. The values of activation free energy (ΔG^*) and activation entropy (ΔS^*) were obtained through the relationships, $\Delta G^* = E_a - RT - T\Delta S^*$ and $\Delta S^* = [\ln A - 1 - \ln(k_B T/h)]/R$ where k_B and h are Boltzmann's and Planck's.

3. Results and discussion

3.1. The formulation of the complexes

o-(Thioalkyl)phenyldiazonium ion is coupled with imidazole in sodium carbonate solution to synthesise 2-((*o*-thioalkyl)pheny-



Scheme 1. The ligands and the complexes.

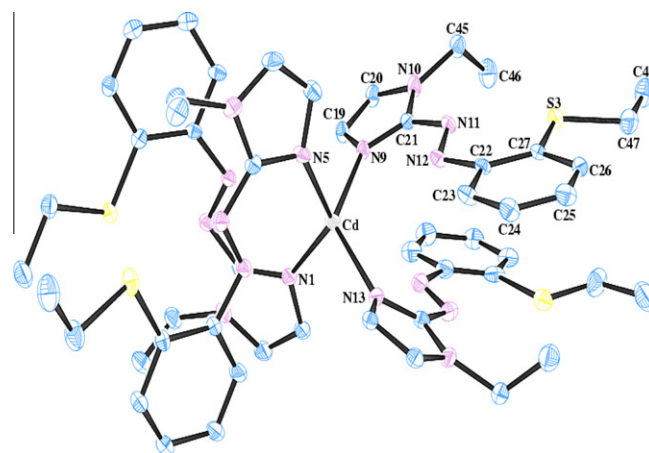


Fig. 2. ORTEP diagram of $[\text{Cd}(\text{SEtaiiNEt})_4](\text{ClO}_4)_2$ (**6d**) with 30% atomic probability (for clarity we have used to label all atoms of one of the four similar ligands and hydrogen atoms are omitted).

Table 2
Selected bond distances and bond angles of $[\text{Cd}(\text{SEtaiiEt})_2]_2$ (**5d**).

Bond lengths (Å)		Bond angles (°)	
Cd(1)–I(1)	2.7670(9)	I(1)–Cd(1)–I(2)	109.85(2)
Cd(1)–I(2)	2.7554(7)	I(1)–Cd(1)–N(2)	97.06(12)
Cd(1)–N(2)	2.251(5)	I(1)–Cd(1)–N(2')	110.12(13)
Cd(1)–N(2')	2.253(5)	I(2)–Cd(1)–N(2)	106.24(12)
N(3)–N(4)	1.264(6)	I(2)–Cd(1)–N(2')	99.15(13)
N(3')–N(4')	1.278(7)	N(2)–Cd(1)–N(2')	133.52(17)

Table 3
Selected bond distances (Å) and angles (°) for $[\text{Cd}(\text{SEtaiiNEt})_4](\text{ClO}_4)_2$ (**6d**).

Bond distances (Å)		Bond angles (°)	
Cd–N(1)	2.250(5)	N(1)–Cd–N(9)	98.50(17)
Cd–N(5)	2.279(5)	N(1)–Cd–N(5)	130.22(18)
Cd–N(9)	2.241(4)	N(1)–Cd–N(13)	103.67(16)
Cd–N(13)	2.269(4)	N(1)–Cd–N(16)	83.34(17)
N(3)–N(4)	1.261(5)	N(9)–Cd–N(16)	79.70(16)
N(7)–N(8)	1.270(6)	N(5)–Cd–N(13)	100.32(16)
N(11)–N(12)	1.254(5)	N(9)–Cd–N(5)	96.85(16)
N(15)–N(16)	1.169(4)	N(9)–Cd–N(13)	131.84(16)
Cl(1)–O(1)	1.355(6)	N(1)–Cd–N(8)	80.62(15)
Cl(1)–O(2)	1.308(7)	N(13)–Cd–N(8)	78.50(15)
Cl(1)–O(3)	1.273(8)	N(5)–Cd–N(8)	62.36(15)
Cl(2)–O(5)	1.383(9)	N(16)–Cd–N(8)	131.49(15)
Cl(2)–O(6)	1.421(12)	N(13)–Cd–N(16)	61.45(17)

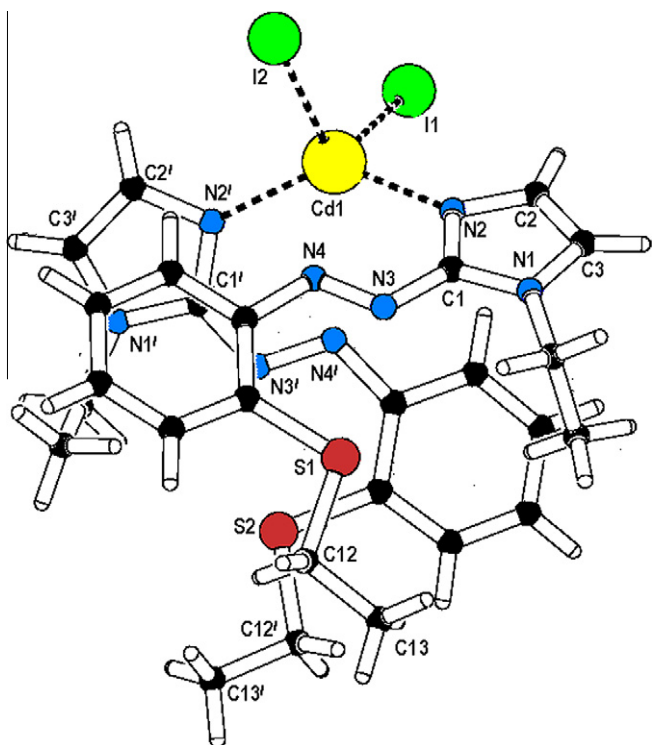
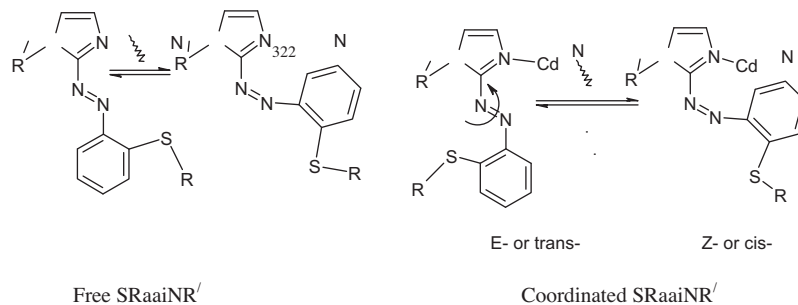


Fig. 1. Crystal structure of $[\text{Cd}(\text{SEtaiiNEt})_2]_2$ (**5d**).

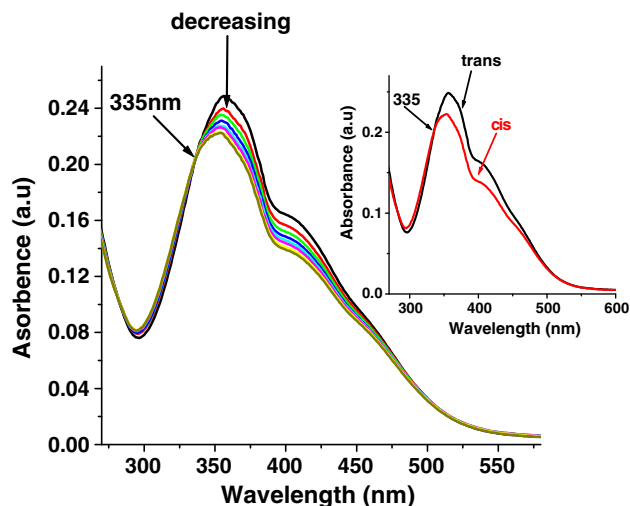
lazoimidazole. It is then undergone alkylation by adding alkyl iodide (MeI, EtI) in dry THF solution in presence of NaH to synthesise 1-alkyl-2-((*o*-thioalkyl)phenylazo)imidazoles [$\text{SRAaiNR}'$ ($\text{R}=\text{R}'=\text{Me}$ (**2a**); $\text{R}=\text{Me}$, $\text{R}'=\text{Et}$ (**2b**); $\text{R}=\text{Et}$, $\text{R}'=\text{Me}$ (**2c**); $\text{R}=\text{R}'=\text{Et}$ (**2d**)). The compounds are then purified by column chromatography.

The reaction of CdX_2 ($\text{X}=\text{Cl}$, Br , I) with $\text{SRAaiNR}'$ in CH_3CN (1:2 mol proportion) isolates dark coloured crystalline compounds of composition $[\text{Cd}(\text{SRAaiNR}')_2\text{X}_2]$ (**3–5**). The reaction of $\text{Cd}(\text{ClO}_4)_2 \cdot 6\text{H}_2\text{O}$ with $\text{SRAaiNR}'$ in CH_3CN has synthesized $[\text{Cd}(\text{SRAaiNR}')_4](\text{ClO}_4)_2$ (**6**). The composition of the complexes has been confirmed by microanalytical data and by other spectroscopic information. The structures have been established in representative cases by single-crystal X-ray diffraction studies.

The IR spectra of the complexes in KBr disc show moderately intense stretching at 1620–1650 and 1415–1430 cm^{-1} and are assigned to $\nu(\text{C}=\text{N})$ and $\nu(\text{N}=\text{N})$, respectively. The $\nu(\text{ClO}_4)$ appears at 1110–1100 and 1080–1085 cm^{-1} defining less symmetric tetrahedral symmetry of hydrogen bonded ClO_4^- ion [22]. Other vibrations are shifted to lower frequency in the complexes compared to the free ligand values [23].



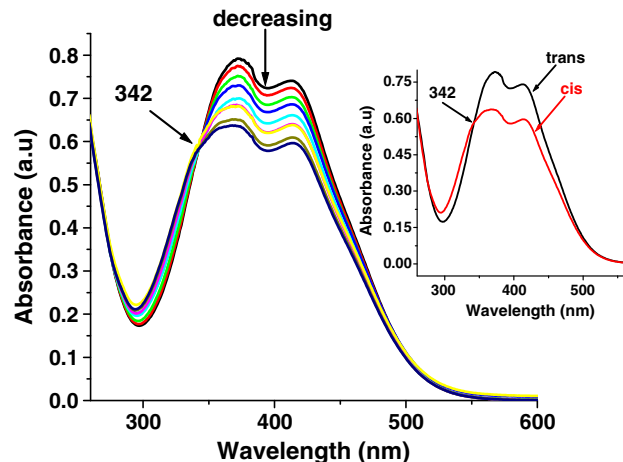
Scheme 2. Photochromism of free and coordinated SRAaiNR.

Fig. 3. Spectral changes due to *E* → *Z* isomerisation of SetaaiNEt in MeCN upon repeated irradiation at 357 nm at 3 min interval at 25 °C.

The ^1H NMR spectra of complexes are recorded in CDCl_3 and the signals are assigned unambiguously *via* spin–spin interaction, the effect of substitutions therein, and on comparing the reported cases [6,7]. The atom numbering pattern is shown in the Scheme 1. Imidazolyl 4- and 5-H show broad singlet at 7.4 and 7.2 ppm, respectively for the complexes $[\text{Cd}(\text{SRAaiNR}')_2\text{X}_2]$ (**3–5**) and are downfield shifted by 0.1–0.2 ppm compared to free ligand data [6]. The broadening may be considered of rapid proton exchange between these imidazole protons and/or exchange with solvent proton. The complexes $[\text{Cd}(\text{SRAaiNR}')_4](\text{ClO}_4)_2$ (**6**) show $\delta(4\text{-H})$ and $\delta(5\text{-H})$ at 7.1 and 6.9 ppm, respectively. The coordination of four bulky SRAaiNR' to Cd(II) may reduce the bonding interaction between metal ion and imidazole-N and causes insufficient downfield shift. Phenyl protons (8- to 11-H) of $-\text{S}(\text{R})-\text{C}_6\text{H}_4$ remain almost unperturbed. This spectral information supports the single crystal structures given in Figs. 1 and 2 where SRAaiNR' act as monodentate imidazolyl-N donor ligand. The N(1)–Me appears as singlet at *ca.* 4.2 ppm; N–CH₂–CH₃ shows a quartet for –CH₂– at *ca.* 4.5 (7 Hz) and a triplet at *ca.* 1.6 (7 Hz) ppm. The thioalkyl group S–R also exhibits a singlet signal at 2.6 ppm for S–Me of SMeaiNR' (**3a,b–6a,b**). SetaaiNEt (**3d–6d**) shows two quartets [4.5 (7 Hz) and 3.00 (7 Hz) ppm for –CH₂– protons of N–CH₂–(CH₃) and S–CH₂–CH₃, respectively] and two triplets [at 1.6 (7 Hz) and 1.3 (6 Hz) ppm for –(N–CH₂)–CH₃ and –(S–CH₂)CH₃, respectively].

3.2. Molecular structures of $[\text{Cd}(\text{SEtaiNEt})_2\text{I}_2]$ (**5d**) and $[\text{Cd}(\text{SEtaiNEt})_4](\text{ClO}_4)_2$ (**6d**)

The molecular structures of $[\text{Cd}(\text{SEtaiNEt})_2\text{I}_2]$ (**5d**) and $[\text{Cd}(\text{SEtaiNEt})_4](\text{ClO}_4)_2$ (**6d**) are shown in Figs. 1 and 2, respec-

Fig. 4. Spectral changes of *E* (*trans*) → *Z* (*cis*) isomerisation of coordinated SetaaiNEt at $[\text{Cd}(\text{SEtaiNEt})_2\text{I}_2]$ (**5d**) in MeCN upon repeated irradiation at 372 nm at 3 min interval at 25 °C.

tively. The bond parameters are given in Tables 2 and 3. The structure of **5d** shows the CdN_2I_2 coordination sphere and that of **6d** is CdN_4 those are arranged in a distorted tetrahedral geometry. 1-Ethyl-2-((*o*-thioethyl)phenylazo)imidazole (SEtaiNEt) has three donor centres imidazolyl-N, azo-N and –S-Et. The structures (Figs. 1 and 2) show that SetaaiNEt hooks to Cd(II) by imidazolyl-N donor centre and two other centres are freely hanging. The examples of metal complexes where SRAaiNR' act as tridentate [6] and didentate [7] are known; however, monodentate coordination complexes are scarce [4]. Uncoordinated donor centres in the multidentate ligands are important for the execution of metallo-ligand activity and synthesis of multimetallic complexes [24] for different reasons like catalyses [25]. Four Cd–N(imidazole) bond lengths in **6d** are unequal and spanning 2.241–2.279 Å. Forced chelation of N(azo) to Cd(II) shows appreciably long bond distance in the complexes; the Cd···N(azo) lengths in **5d** are Cd–N(4), 2.831(2); Cd–N(4'), 2.958(4) Å and in **6d** are Cd···N(4), 2.988; Cd···N(12), 3.009 Å. The sum of the van der Waals radii, Cd···N(sp^2) is 3.13 Å [26] and the chelate angle, N(imidazole)–Cd–N(azo) [N(2)–Cd–N(4), 68.72(1); N(2')–Cd–N(4') 61.21(4)°] is smaller than previous report [10] which has supposed to conclude the no chelation of N(azo)/–S-Et. The preferential bonding of imidazolyl-N to Cd(II) supports the strong toxicity of Cd(II) [27] because imidazole is an integral component of most of the biomolecules. The imidazolyl group is deviated by 24° from the plane of phenyl-thioalkyl group. Two ligands of coordinated SetaaiNEt in **5d** make a dihedral angle 78.4(6)°. The coordination environment about Cd in **6d** is compressed along the crystallographic *c*-axis in such a way that two of the N–Cd–N angles are lower than tetrahedral angle with a value of N(1)–Cd–N(9), 98.50(17) and N(5)–Cd–N(13), 100.32(16)°. Two other N–Cd–N angles show higher value [N(1)–Cd–N(5),

Table 4
Excitation wavelength (λ_{π, π^*}), rate of E (*trans*) \rightarrow Z (*cis*) conversion and quantum yield ($\Phi_{E \rightarrow Z}$).

Compound	λ_{π, π^*} (nm)	Isobastic points (nm)	Rate of $E \rightarrow Z$ conversion $\times 10^8$ (s $^{-1}$)	($\Phi_{E \rightarrow Z}$).
SMeaiNMe (2a) ^a	357	337	4.908	0.317
SMeaiNEt (2b) ^a	358	337	3.108	0.232
SEtaaiNMe (2c) ^a	357	336	4.67	0.290
SEtaaiNEt (2d) ^a	356	335	2.948	0.197
[Cd(SMeaiNMe) ₂ Cl ₂] (3a)	372	344	0.687	0.060
[Cd(SMeaiNEt) ₂ Cl ₂] (3b)	372	342	0.631	0.054
[Cd(SEtaaiNMe) ₂ Cl ₂] (3c)	373	343	0.639	0.055
[Cd(SEtaaiNEt) ₂ Cl ₂] (3d)	371	339	0.568	0.049
[Cd(SMeaiNMe) ₂ Br ₂] (4a)	371	338	0.728	0.072
[Cd(SMeaiNEt) ₂ Br ₂] (4b)	372	339	0.678	0.063
[Cd(SEtaaiNMe) ₂ Br ₂] (4c)	373	336	0.681	0.067
[Cd(SEtaaiNEt) ₂ Br ₂] (4d)	373	335	0.625	0.057
[Cd(SMeaiNMe) ₂ I ₂] (5a)	373	342	1.416	0.158
[Cd(SMeaiNEt) ₂ I ₂] (5b)	372	350	1.221	0.121
[Cd(SEtaaiNMe) ₂ I ₂] (5c)	371	341	1.255	0.133
[Cd(SEtaaiNEt) ₂ I ₂] (5d)	372	342	1.012	0.076
[Cd(SMeaiNMe) ₄](ClO ₄) ₂ (6a)	371	340	0.582	0.047
[Cd(SMeaiNEt) ₄](ClO ₄) ₂ (6b)	373	337	0.532	0.037
[Cd(SEtaaiNMe) ₄](ClO ₄) ₂ (6c)	372	338	0.541	0.040
[Cd(SEtaaiNEt) ₄](ClO ₄) ₂ (6d)	371	336	0.487	0.027

^a Data are obtained from Ref. [17].

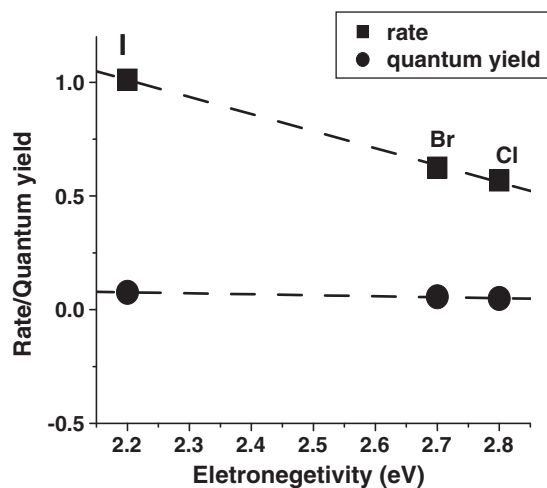


Fig. 5. Effect of electronegativity of X in [Cd(SEtaaiNEt)₂X₂] on rate and quantum yield of photoisomerisation.

130.22(18) and N(9)–Cd–N(13), 131.84(16)°). The angular distortion from regular tetrahedron geometry may be due to steric crowding among the pendant thioethylphenylazo groups. Out of four –N=N– distances of 6d three lengths (N(3)–N(4), 1.261(5); N(7)–N(8), 1.270(6); N(11)–N(12), 1.254(5) Å) are comparable to the published results [8–11]. The N(15)–N(16) is 1.169(6) Å but not unusual since similar observation is reported in case of ionic compounds such as [MeaiH₂(H₂O)⁺]₂[PtCl₆]²⁻:N=N 1.214(8), 1.197(11) Å [28].

The packing of crystal (**5d**) shows recognisable weak interactions such as Cg(1)··Cg(1'), 3.386(2) Å (where Cg(1): N(1), C(1), N(2), C(2), C(3); and Cg(2): N(1'), C(1'), N(2'), C(2'), C(3')); symmetry code: 2-x, 1-y, 2-z) and C(5)–H(5)··Cg(1') (H(5)··Cg(1'), 2.979(2) Å; C(5)··Cg(1'), 3.336(4) Å and ∠C(5)–H(5)··Cg(1'), 103.7(8)°). In **6d**, ClO₄⁻ bridges two complex units of [Cd(SEtaaiNEt)₄]²⁺ via hydrogen bonds to imidazolyl group (C–H(30)) and imidazolyl-N-CH₂-CH₃ (C–H(42a)) of neighbouring molecule [C–H(30)··O(ClO₄)O··H(42a)–C: H(30)··O, 2.51; C(30)··O, 3.4083; ∠C–H(30)··O, 162°; H(42a)··O, 2.54; C(42)··O, 3.2425; ∠C–H(42a)··O, 130°)

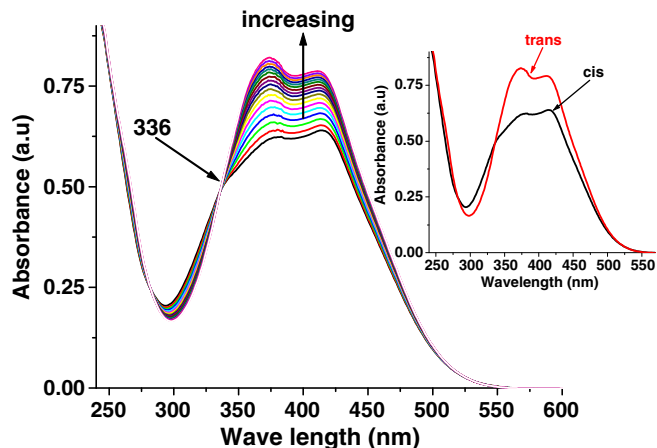


Fig. 6. Spectral changes during Z (*cis*) \rightarrow E (*trans*) isomerisation of [Cd(SEtaaiNEt)₂I₂] (**5d**) in MeCN solution at 298 K. Z -isomer is generated by irradiation of UV light for 45 min and allowed to thermal isomerisation. Inset picture shows spectral change of individual isomer.

3.3. UV-Vis spectra and photochromism

The solution electronic spectra of the compounds were recorded in CH₃CN in 200–600 nm. There are two bands in the UV-Vis region at 360–380 and 410–416 nm. The E -to- Z (*trans*-to-*cis*) isomerisation of the complexes (Scheme 2) has been investigated by irradiation of UV light in acetonitrile solution (Fig. 3) and has also compared with free ligand spectral changes (Fig. 4). Absorption spectra of the E -configuration of coordinated SRaiiNR in the complexes, **3–6**, in CH₃CN are changing with isobestic point upon excitation to the *cis* configuration of the ligand. The complexes show little degradation upon repeated irradiation at least up to 15 cycles in each case that has been verified by measuring absorbance before and after irradiation at $\pi \rightarrow \pi^*$ band. The quantum yields were measured for the E -to- Z ($\Phi_{E \rightarrow Z}$) photoisomerisation of these compounds in CH₃CN on irradiation of UV wavelength (Table 4). The $\Phi_{E \rightarrow Z}$ values are significantly dependent on the nature of the substituents, halide type and molecular weight [29]. In presence of –Me and –Et group quantum yield values reduce in both cases compare to free ligands.

Table 5
Rate and activation parameters for *Z* (*cis*) → *E* (*trans*) thermal isomerisation.

Compd	Temp (K)	Rate of thermal <i>Z</i> → <i>E</i> conversion × 10 ⁴ (s ⁻¹)	<i>E</i> _a (kJ mol ⁻¹)	Δ <i>H</i> [*] (kJ mol ⁻¹)	Δ <i>S</i> [*] (J mol ⁻¹ K ⁻¹)	Δ <i>G</i> [*] (kJ mol ⁻¹)
2a^a	298	4.329	25.42	22.88	-232.41	92.13
	303	5.295				93.29
	308	6.191				94.45
	313	7.091				95.62
2b^a	298	4.614	22.99	20.45	-240.02	91.97
	303	5.598				93.17
	308	6.293				94.37
	313	7.269				95.57
2c^a	298	4.425	21.92	19.38	-244.04	92.11
	303	5.123				93.33
	308	5.985				94.55
	313	6.729				95.77
2d^a	298	4.625	18.88	16.34	-253.96	92.02
	303	5.123				93.29
	308	5.985				94.56
	313	6.589				95.83
3a	306	5.801	18.82	16.22	-254.06	77.76
	311	6.599				79.03
	316	7.31				80.23
	321	8.232				81.57
3b	306	6.081	16.44	13.84	-261.48	80.026
	311	6.789				81.33
	316	7.322				82.64
	321	8.296				83.95
3c	306	6.121	17.22	14.62	-258.90	79.24
	311	6.809				80.53
	316	7.47				81.83
	321	8.436				83.12
3d	306	6.416	13.69	11.09	-270.01	82.63
	311	7.088				83.98
	316	7.512				85.33
	321	8.322				86.68
4a	306	5.99	19.80	17.2	-250.61	76.71
	311	6.798				77.96
	316	7.688				79.21
	321	8.612				80.46
4b	306	6.151	18.93	16.33	-253.29	77.52
	311	6.852				78.79
	316	7.719				80.06
	321	8.701				81.32
4c	306	6.171	19.01	16.4	-253.01	77.44
	311	6.899				78.70
	316	7.749				79.97
	321	8.751				81.23
4d	306	6.457	14.78	12.18	-266.33	81.51
	311	7.312				82.84
	316	7.65				84.17
	321	8.6				85.50
[Cd(SMeaaiNMe) ₂] ₂ (5a)	306	5.847	21.83	19.22	-249.41	76.34
	311	6.660				77.59
	316	7.654				78.83
	321	8.715				80.08
5b	306	6.089	19.599	16.7	-251.21	76.89
	311	6.799				78.14
	316	7.64				79.4
	321	8.74				80.65
5c	306	6.1	19.92	17.32	-250.14	76.56
	311	6.841				77.81
	316	7.722				79.06
	321	8.799				80.32
5d	306	6.395	15.37	12.76	-264.49	80.95
	311	7.259				82.27
	316	7.622				83.59
	321	8.61				84.92
6a	306	5.917	17.61	15.01	-257.90	78.93
	311	6.599				80.22
	316	7.251				81.51
	321	8.216				82.80
6b	306	6.195	14.50	12.39	-266.09	81.43
	311	6.783				82.76
	316	7.246				84.1
	321	8.234				85.43
6c	306	6.201	15.24	12.64	-265.26	81.18
	311	6.833				82.51

(continued on next page)

Table 5 (continued)

Compd	Temp (K)	Rate of thermal Z → E conversion × 10 ⁴ (s ⁻¹)	E _a (kJ mol ⁻¹)	ΔH [‡] (kJ mol ⁻¹)	ΔS [‡] (J mol ⁻¹ K ⁻¹)	ΔG [‡] (kJ mol ⁻¹)
6d	316	7.296	12.14	9.54	-275.01	83.83
	321	8.284				85.16
	306	6.484				84.16
	311	6.996				85.54
	316	7.464				86.91
	321	8.131				88.29

^a Data are obtained from Ref. [17].

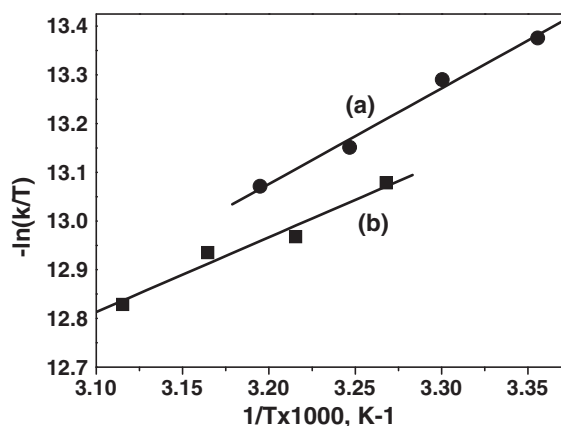


Fig. 7. The Eyring plots of rate constants of Z-to-E thermal isomerisation of SEtaaiNET (O) and [Cd(SEtaaiNEt)₂I₂] (5d) (■) at different temperatures.

Upon UV light irradiation *trans* (E) structure of SRaaiNR' changes to *cis* (Z) structure about the azo (-N=N-) function and the *cis* molar ratio has reached to >80% (Scheme 2). UV-light irradiation to the solution of the photochrome may insist the rotation of the azo-aryl group (-N=N-Ar) which isomerizes from *trans* (E) to *cis* (Z) form. The rates of photoisomerisation (*trans*-to-*cis* (E-Z), $\phi_{E \rightarrow Z}$) increases with decreasing electronegativity of X in the complexes (Fig. 5); rate follows [Cd(SRaaiNR')₂Cl₂] (3) < [Cd(SRaaiNR')₂Br₂] (4) < [Cd(SRaaiNR')₂I₂] (5) although the molar mass follows the order 3 < 4 < 5. Higher electronegativity of Cl in 3 may help to enhance association strength by electrostatic interaction with neighbouring molecules and may effectively increase rotor mass than that of 4 or 5.

The Z-to-E (*cis*-to-*trans*) isomerisation at thermal condition was followed by UV-Vis spectroscopy (Fig. 6) in MeCN at varied temperatures, 306–316 K and the activation energies were obtained (Table 5) from the Eyring plots (Fig. 7). In the complexes the E_as are quite closer to respective free ligands, which mean slow rate of Z-to-E thermal isomerisation of the complexes. The entropies of activation (ΔS[‡]) are more negative in the complexes than that of the free ligands. This is also defending the increase in rotor volume in the complexes.

The complexes have available pendant N, S-coordination centres. The pendant arms bearing additional coordinating groups in a metal complex have several advantages and are useful in many different chemical applications such as catalysis [30], selective cation binding [30,31], mimicry of enzymes and siderophores [32]. The impact of metal coordination on the photoisomerisation of the [Cd(SRaaiNR')₂X₂] and [Cd(SRaaiNR')₄](ClO₄)₂ are examined. The addition of Cd(ClO₄)₂ solution (in MeCN, 10⁻⁴ M) followed by UV light irradiation has shown the quenching of photoisomerisation. The coordination of Cd(II) to the pendant N,S-coordination centres may increase rotor mass and may inhibit the photoisomerisation of the chromophore. The progress of the work is under investigation.

4. Conclusion

Two series of Cd(II)-1-alkyl-2-((*o*-thioalkyl)phenylazo)imidazole (SRaaiNR') complexes are described: [Cd(SRaaiNR')₂X₂] (X = Cl, Br, I) and [Cd(SRaaiNR')₄](ClO₄)₂. The crystal structures of the complexes have shown monodentate, N(imidazole), nature of SRaaiNR' although they have three donor centres N(imidazole), N(azo) and -SR. Photochromism of the complexes are examined by UV light irradiation in CH₃CN solution. Rate of photoisomerisation and quantum yields are decreased in the complexes compared with free ligands data. The decrease in electronegativity of X increases the rate of E-to-Z photoisomerisation. The Z-to-E isomerisation is thermally driven process. The activation energy (E_as) of Z-to-E isomerisation has been calculated. The slow rate of isomerisation in complexes may be due to higher rotor volume than that of free ligands.

Acknowledgements

Financial support from Department of Science & Technology, New Delhi is thankfully acknowledged. Our sincere thanks due to Mr. Rajat Saha, Department of Physics, Jadavpur University for help in crystallographic work.

Appendix A. Supplementary data

CCDC 865742 and 654229 contain the supplementary crystallographic data for [Cd(SEtaaiNEt)₂I₂] (5d) and [Cd(SEtaaiNEt)₄](ClO₄)₂ (6d), respectively. These data can be obtained free of charge via <http://www.ccdc.cam.ac.uk/conts/retrieving.html>, or from the Cambridge Crystallographic Data Centre, 12 Union Road, Cambridge CB2 1EZ, UK; fax: (+44) 1223-336-033; or e-mail: deposit@ccdc.cam.ac.uk.

References

- [1] F.A. Cotton, G. Wilkinson, C.A. Murillo, M. Bochmann, *Advanced Inorganic Chemistry*, sixth ed., Wiley-Interscience, New York, 1999.
- [2] M.J. Scoullon, G.H. Vonkeman, I. Thornton, Z. Makuch, Mercury, Cadmium, Lead: Handbook for Sustainable Heavy Metals Policy and Regulation, Springer, 2001.
- [3] J.A. Christopher, A.K. Mukhtar, A. Guy Orpen, *Inorg. Chem.* 49 (2010) 10475.
- [4] B.G. Chand, U.S. Ray, J. Cheng, J. Cheng, T.-H. Lu, C. Sinha, *Inorg. Chim. Acta* 358 (2005) 1927.
- [5] U.S. Ray, D. Banerjee, G. Mostafa, T.-H. Lu, C. Sinha, *New J. Chem.* 28 (2004) 1432.
- [6] D. Banerjee, U.S. Ray, Sk. Jasimuddin, J.-C. Liou, T.-H. Lu, C. Sinha, *Polyhedron* 25 (2006) 1299.
- [7] G. Saha, P. Datta, K.K. Sarker, R. Saha, G. Mostafa, C. Sinha, *Polyhedron* 30 (2011) 614.
- [8] J. Otsuki, K. Suwa, K. Narutaki, C. Sinha, I. Yoshikawa, K. Araki, *J. Phys. Chem. A* 109 (2005) 8064.
- [9] J. Otsuki, K. Suwa, K.K. Sarker, C. Sinha, *J. Phys. Chem. A* 111 (2007) 1403.
- [10] K.K. Sarker, D. Sardar, K. Suwa, J. Otsuki, C. Sinha, *Inorg. Chem.* 46 (2007) 8291.
- [11] P. Pratihar, T.K. Mondal, A.K. Patra, C. Sinha, *Inorg. Chem.* 48 (2009) 2760.
- [12] C.V. Yelamaggad, I. Shashikala, U.S. Hiremath, D.S.S. Rao, S.K. Prasad, *Liq. Cryst* 34 (2007) 153.
- [13] S. Kawata, Y. Kawata, *Chem. Rev* 100 (2000) 1777.
- [14] E. Katz, A.N. Shipway, I. Willner, in: Z. Sekkat, W. Knoll (Eds.), *Photoreactive Organic Films*, Academic, San Diego, 2002, p. 220.

- [15] M. Irie (Ed.), Photochromism: memories and switches, Chem. Rev. 100 100 (2000) 1683 (special issue).
- [16] J.C. Crano, R.J. Guglielmetti (Eds.), Organic Photochromic and Thermochromic Compounds, Kluwer Academic/Plenum Publishers, New York, NY, 1999.
- [17] G.M. Sheldrick, SHELXS-97, University of Gottingen, Germany, 1997.
- [18] G.M. Sheldrick, SHELXL 97, University of Gottingen, Germany, 1997.
- [19] J. Farrugia, J. Appl. Cryst. 30 (1997) 565.
- [20] A.L. Spek, PLATON, The Netherlands (1999).
- [21] G. Zimmerman, L. Chow, U. Paik, J. Am. Chem. Soc. 80 (1958) 3528.
- [22] R. Gupta, S. Mukherjee, R. Mukherjee, J. Chem. Soc., Dalton Trans. (1999) 4025.
- [23] T.K. Misra, Ph. D. thesis, (1999).
- [24] S. Pal, T. Melton, R.N. Mukherjee, A.R. Chakravarty, M. Tomas, L.R. Falvello, A. Chakravorty, Inorg. Chem. 24 (1985) 1250.
- [25] M.C. Das, S. Xiang, Z. Zhang, B. Chen, Angew. Chem., Int. Ed. Engl. 50 (2011) 10510.
- [26] <http://www.webelements.com/cadmium/atom_sizes.html>.
- [27] J.E. Fergusson, The Heavy Elements: Chemistry, Environment Impact And Health Effects, Pergamon, Oxford, 1990.
- [28] S.S. Halder, G. Saha, B.G. Chand, A.D. Jana, G. Mostafa, J. Cheng, T.-H. Lu, C. Sinha, Inorg. Chim. Acta 363 (2010) 2080.
- [29] H. Nishihara, Bull. Chem. Soc. Jpn. 77 (2004) 407.
- [30] R. Reichenbach-Klinke, B. Knöig, Dalton Trans. (2002) 121.
- [31] T. Koike, T. Abe, M. Takahashi, K. Ohtani, E. Kimura, M. Shiro, Dalton Trans. (2002) 1764.
- [32] T. Tanase, H. Inukai, T. Onaka, M. Kato, S. Yano, S.J. Lippard, Inorg. Chem. 40 (2001) 3943.